

## Second Hyperpolarizabilities of Singlet Polycyclic Diphenalenyl Radicals: Effects of the Nature of the Central Heterocyclic Ring and Substitution to Diphenalenyl Rings

Masayoshi Nakano,<sup>\*,†</sup> Nozomi Nakagawa,<sup>†</sup> Ryohei Kishi,<sup>†</sup> Suguru Ohta,<sup>†</sup> Masahito Nate,<sup>†</sup> Hideaki Takahashi,<sup>†</sup> Takashi Kubo,<sup>‡</sup> Kenji Kamada,<sup>§</sup> Koji Ohta,<sup>§</sup> Benoît Champagne,<sup>⊥</sup> Edith Botek,<sup>⊥</sup> Yasushi Morita,<sup>‡</sup> Kazuhiro Nakasuji,<sup>‡</sup> and Kizashi Yamaguchi<sup>‡</sup>

Department of Materials Engineering Science, Graduate School of Engineering Science, Osaka University, Toyonaka, Osaka 560-8531, Japan, Department of Chemistry, Graduate School of Science, Osaka University, Toyonaka, Osaka 560-0043, Japan, Photonics Research Institute, National Institute of Advanced Industrial Science and Technology (AIST), Ikeda, Osaka 563-8577, Japan, and Laboratoire de Chimie Théorique Appliquée, Facultés Universitaires Notre-Dame de la Paix (FUNDP), rue de Bruxelles, 61, B-5000 Namur, Belgium

Received: May 7, 2007; In Final Form: July 19, 2007

Adopting density functional theory and a hybrid exchange-correlation functional, the relationship between the second hyperpolarizability ( $\gamma$ ) and the diradical character has been investigated for diphenalenyl-based compounds containing different heterocyclic five-membered central rings ( $C_4H_4X$ , where  $X = NH, PH, O, S, CH_2, SiH_2, BH, GaH, C=O, C=S, \text{ and } C=Se$ ) or substituted by donor ( $NH_2$ )/acceptor ( $NO_2$ ) groups. It turns out that these structural modifications can tune the diradical character from 0.0 to 0.968 and lead to variations of  $\gamma$  over more than 1 order of magnitude, demonstrating the controllability of  $\gamma$  in this family of compounds. In particular, when the central ring is strongly aromatic, the diradical character is larger than 0.7, which is associated with pretty large  $\gamma$  values except for almost the pure diradical case ( $\gamma \approx 1$ ). On the other hand, when the aromaticity decreases—or the antiaromaticity increases—the diradical character and the second hyperpolarizability get smaller. These relationships are correlated to structural (bond length alternation) and charge distribution (charge transfer between the phenalenyl rings and the central ring) properties, which account for the relative importance of the resonance diradical, zwitterionic, and quinoid forms. Therefore, the diradical character and the second hyperpolarizability can be controlled by the aromaticity of the ring while the paradigm of the enhancement of  $\gamma$  for intermediate diradical character is globally verified. Then, upon introducing donor groups, the zwitterionic character increases, leading to closed-shell species and small second hyperpolarizabilities. In the case of substitution by acceptor groups, the charge transfer is reduced but the diradical character and the second hyperpolarizability hardly changes.

### 1. Introduction

Organic compounds presenting large nonlinear optical (NLO) properties have been actively studied both theoretically and experimentally<sup>1–7</sup> in order to build new photonics devices such as optical switches and three-dimensional memories. In particular, the second hyperpolarizabilities ( $\gamma$ )—the molecular response at the origin of the third-order NLO properties—of organic  $\pi$ -conjugated systems have been investigated and several structural and electronic factors have been shown to control the amplitude and sign of  $\gamma$ , e.g., the  $\pi$ -conjugation length, the strength of the donor/acceptor substituents, and the charge state.<sup>8–21</sup> Most systems studied so far, however, have been limited to closed-shell systems. Recently, we have theoretically proposed other tuning parameters for  $\gamma$  of open-shell systems, e.g., the spin multiplicity<sup>22</sup> and the diradical character ( $\gamma$ ).<sup>23,24</sup> Indeed, the  $\gamma$  values of open-shell systems remarkably change with the spin multiplicity<sup>22,24</sup> while singlet  $\pi$ -conjugated systems with intermediate diradical character exhibit a large enhancement

of  $\gamma$  compared to conventional closed-shell  $\pi$ -conjugated systems ( $\gamma \approx 0$ ) and pure diradical systems ( $\gamma \approx 1$ ).<sup>24</sup>

In a previous study,<sup>24f</sup> we have focused on the singlet polycyclic diphenalenyl diradical (DPL) compounds, IDPL, *as*-IDPL, and TDPL, to examine the effects of dominant resonance forms, i.e., *p*- and *o*-quinoid structures, in the middle region of these systems as well as the effect of replacing the central benzene ring by a thiophene ring. For these compounds, the relationship between the diradical character and the  $\gamma$  values is in agreement with our prediction that  $\gamma$  is enhanced in compounds with intermediate diradical character as compared to compounds with small or large diradical characters. Very recently, two-photon absorption (TPA) measurements were carried out on some of these diphenalenyl compounds and it appeared that these systems present the largest TPA cross sections among pure hydrocarbons.<sup>25</sup> These results also suggest the existence of close relationships between the aromaticity of the central five-membered ring and the diradical character, which appear to be useful for tuning the second hyperpolarizability by chemical modification of the structures.

Subsequently, this study addresses the impact of the nature of this central ring on the diradical character and second hyperpolarizability of diphenalenyl compounds. In particular, 11 five-membered rings ( $C_4H_4X$ , where  $X = NH, PH, O, S,$

\* Address correspondence to this author. Fax: +81-6-6850-6268. E-mail: mnaka@cheng.es.osaka-u.ac.jp.

<sup>†</sup> Graduate School of Engineering Science, Osaka University.

<sup>‡</sup> Graduate School of Science, Osaka University.

<sup>§</sup> National Institute of Advanced Industrial Science and Technology.

<sup>⊥</sup> Facultés Universitaires Notre-Dame de la Paix.

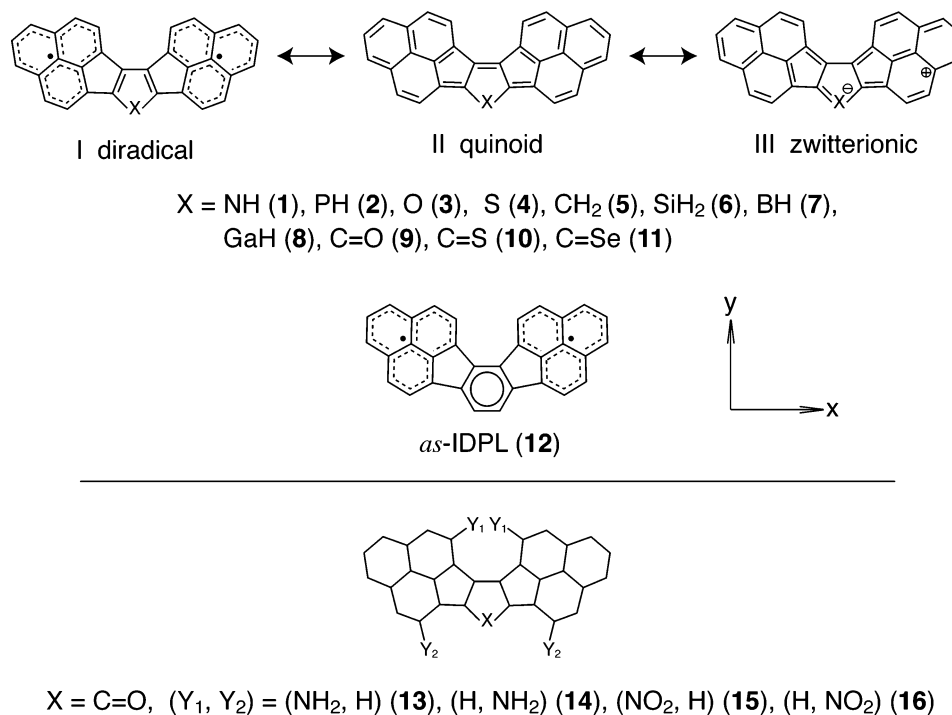


**Figure 1.** Resonance [diradical (I), quinoid (II), and zwitterionic (III)] forms of the singlet ground state of polycyclic diphenalenyl radicals (DPLs) involving five-membered rings covering a large range of aromatic character [C<sub>4</sub>H<sub>4</sub>X, where X = NH (1), PH (2), O (3), S (4), CH<sub>2</sub> (5), SiH<sub>2</sub> (6), BH (7), GaH (8), C=O (9), C=S (10), and C=Se (11)]. Reference molecule, *as*-IDPL, and donor/acceptor-disubstituted derivatives [DPLs with X = C=O, (Y<sub>1</sub>, Y<sub>2</sub>) = (NH<sub>2</sub>, H) (13), (H, NH<sub>2</sub>) (14), (NO<sub>2</sub>, H) (15), (H, NO<sub>2</sub>) (16)] are also shown.

CH<sub>2</sub>, SiH<sub>2</sub>, BH, GaH, C=O, C=S, C=Se) covering a broad range of aromaticity were selected and compared to the reference *as*-IDPL involving a central benzene ring (Figure 1). These investigations are carried out by using density functional theory and a hybrid exchange–correlation functional containing 50% of Hartree–Fock exchange, the BHandHLYP functional. The  $y$  and  $\gamma$  values have been rationalized in terms of aromaticity indices, and precisely using the “nucleus independent chemical shift (NICS)” proposed by von Schleyer and collaborators.<sup>26</sup> In addition, the energy gap between the highest and lowest molecular orbitals (HOMO–LUMO energy gap) is also considered. Then, the effects on  $y$  and  $\gamma$  of substituting the diphenalenyl rings by donor (–NH<sub>2</sub>) and acceptor (–NO<sub>2</sub>) groups have been tackled (Figure 1). On the basis of these results, new relationships between the chemical structures and the second hyperpolarizabilities have been rationalized, in particular those involving the control of the diradical character in diphenalenyl compounds.

## 2. Theoretical and Computational Aspects

**2.1. Molecular Structures and Diradical Character.** Figure 1 shows the structures and coordinate axes of singlet polycyclic diphenalenyl radicals involving five-membered rings [C<sub>4</sub>H<sub>4</sub>X, where X = NH (1), PH (2), O (3), S (4), CH<sub>2</sub> (5), SiH<sub>2</sub> (6), BH (7), GaH (8), C=O (9), C=S (10), C=Se (11)] and *as*-IDPL (12) as well as four kinds of disubstituted derivatives [DPL with X = C=O, (Y<sub>1</sub>, Y<sub>2</sub>) = (NH<sub>2</sub>, H) (13), (H, NH<sub>2</sub>) (14), (NO<sub>2</sub>, H) (15), (H, NO<sub>2</sub>) (16)]. For all systems, the  $x$ -axis is taken to be the direction of the longitudinal axis and the  $x$ – $y$  plane defines the molecular plane (Figure 1). For the donor/acceptor-disubstituted systems 13–16, the positions of substitution correspond to large contributions to the highest occupied molecular orbital (HOMO) and are aligned along the  $y$  direction to favor charge transfer (CT) between the amino donor groups and the carboxy

acceptor group on the central ring and therefore to allow variations of the diradical character. The structures of these systems were optimized at the UB3LYP level of approximation by using the 6-31G\*\* basis set under the constraint of C<sub>2v</sub> symmetry since the B3LYP method is known to reproduce the experimental structures of conjugated diradical systems.<sup>27,28</sup> The possible resonance structures between the diradical (I), quinoid (II), and zwitterionic (III) forms are also shown in Figure 1.

The diradical character was calculated from the spin-unrestricted Hartree–Fock (UHF) calculations. The diradical character  $y_i$  associated with the HOMO– $i$  and LUMO+ $i$  is defined by the weight of the doubly excited configuration in the multiconfigurational (MC)-SCF theory and is formally expressed in the case of the spin-projected UHF (PUHF) theory as<sup>29,30</sup>

$$y_i = 1 - \frac{2T_i}{1 + T_i^2} \quad (1)$$

where  $T_i$  is the orbital overlap between the corresponding orbital pairs<sup>29,30</sup> ( $\chi_{\text{HOMO}-i}$  and  $\eta_{\text{HOMO}-i}$ ) and can also be represented by using the occupation numbers ( $n_i$ ) of the UHF natural orbitals (UNOs):

$$T_i = \frac{n_{\text{HOMO}-i} - n_{\text{LUMO}+i}}{2} \quad (2)$$

The diradical characters  $y_i$  with use of the UNO occupation number take a value between 0 (closed-shell system) and 1 (pure diradical system), respectively.

**2.2. Second Hyperpolarizability and Second Hyperpolarizability Density Analysis.** Following recent investigations,<sup>24</sup> the hybrid BHandHLYP<sup>31</sup> exchange–correlation functional and the 6-31G\* basis set were employed to calculate the longitudinal

**TABLE 1:**  $\gamma$  Values, NICS(1), Diradical Character ( $y$ ), HOMO(H)–LUMO(L) Energy Gaps of the Complete Systems (H–L Gap  $t$ ) of the Related  $p$ -Quinoid Rings (H–L Gap  $p$ ) and of the Related  $o$ -Quinoid Rings (H–L Gap  $o$ ), Average Bond Length Alternations (BLAs), and Mulliken Charges on Phenalenyl Rings for Compounds 1–11 (Including Different X, See Figure 1) in Comparison with *as*-IDPL (12)

X	NH (1)	PH (2)	O (3)	S (4)	CH <sub>2</sub> (5)	SiH <sub>2</sub> (6)	BH (7)
NICS(1) <sup>a</sup> [ppm]	−10.60	−5.97	−9.36	−10.79	−4.82	−1.41	9.24
$y^b$	0.899	0.968	0.731	0.768	0.414	0.397	0.374
H–L gap $t^c$ [eV]	2.99	3.35	4.98	2.42	6.28	6.35	6.25
H–L gap $p^c$ [eV]	9.81	9.05	10.11	9.91	10.54	10.60	10.00
H–L gap $o^c$ [eV]	7.19	7.46	6.36	5.89	5.01	5.33	7.62
average BLA [Å]	0.018	0.015	0.023	0.019	0.036	0.035	0.034
charge	0.12	0.12	0.14	0.16	0.09	0.17	0.18
$\gamma^d$ [ $\times 10^3$ au]	1555	827	1934	1349	1202	1286	415
	GaH (8)	C=O (9)	C=S (10)	C=Se (11)	( <i>as</i> -IDPL) (12)		
NICS(1) <sup>a</sup> [ppm]	3.18	2.81	3.46	3.79	−11.26		
$y^b$	0.350	0.367	0.0	0.0	0.923		
H–L gap $t^c$ [eV]	6.35	6.32	6.22	6.19	3.31		
H–L gap $p^c$ [eV]	9.17	10.60	8.87	8.44	9.29		
H–L gap $o^c$ [eV]	6.20	6.56	5.84	5.47	8.83		
average BLA [Å]	0.034	0.035	0.034	0.034	0.013		
charge	0.08	0.21	0.25	0.26	0.07		
$\gamma^d$ [ $\times 10^3$ au]	273	438	98	88	472		

<sup>a</sup> NICS(1) values of five-membered rings are quoted from ref 37 and that of benzene is calculated by the same method, GIAO/HF/6-311+G\*\* method, using the optimized geometry at the MP2(fc)/6-311+G\*\* level of approximation. <sup>b</sup> The  $y$  values are calculated with the UNO/6-31G\* method. <sup>c</sup> The H–L gaps are determined by using the RHF/6-31G\* method. The geometry of the  $p$ -quinoid and  $o$ -quinoid central rings were also optimized at the UB3LYP/6-31G\*\* level of approximation. <sup>d</sup> The  $\gamma$  values are calculated by the (U)BHandHLYP/6-31G\* method.

component of static  $\gamma$  ( $\gamma_{xxx}$ ), which dominates the response in  $\pi$ -conjugated systems. This standard basis set is indeed sufficient to provide semiquantitative  $\gamma$  values—and therefore to allow comparison between systems with different diradical character—though 6-31+G\*-like basis sets are necessary for obtaining quantitative  $\gamma$  values for  $\pi$ -conjugated systems.<sup>32–34</sup> In fact, for a polycyclic diphenalenyl radical, IDPL, adding a set of diffuse p [ $\zeta = 0.0523$  on carbon (C) atoms] functions affects  $\gamma$  by only 10%.<sup>24d</sup> Moreover, as seen from our previous studies on the  $p$ -quinodimethane,<sup>24a</sup> twisted ethylene,<sup>24a</sup> and H<sub>2</sub><sup>23,24b</sup> models, the spin-unrestricted BHandHLYP (UBHandHLYP) method provides reliable  $\gamma$  values for the singlet diradical systems with intermediate and large diradical characters, whereas the spin-restricted BHandHLYP (RBHandHLYP) method provides reliable  $\gamma$  values for the diradical systems with small diradical character or closed-shell systems, at least for the size investigated in this study.

The  $\gamma$  values are determined by using the finite-field (FF) approach,<sup>35</sup> which consists of a fourth-order differentiation of energy with respect to different amplitudes of the applied external electric field. A power series expansion convention (called B convention<sup>36</sup>) is chosen for defining  $\gamma$ . The following fourth-order numerical differentiation formula is employed:

$$\gamma = \frac{1}{36(F)^4} \{E(3F) - 12E(2F) + 39E(F) - 56E(0) + 39E(-F) - 12E(-2F) + E(-3F)\} \quad (3)$$

Here,  $E(F)$  indicates the total energy in the presence of static electric field  $F$ .  $F$  values ranging from 0.0010 to 0.0030 au were used in combination with an accuracy on the energy of  $10^{-10}$  au in order to obtain  $\gamma$  values with sufficient precision for the present study. The  $\gamma$  values are given in atomic units (au): 1.0 au of second hyperpolarizability is equal to  $6.235377 \times 10^{-65}$  C<sup>4</sup> m<sup>4</sup> J<sup>-3</sup> and  $5.0367 \times 10^{-40}$  esu. All calculations are performed with the Gaussian 03 program package.<sup>31</sup>

The spatial contribution of electrons to  $\gamma$  is described by using the  $\gamma$  density analysis.<sup>10,23a,24</sup> The  $\gamma$  density,  $\rho^{(3)}(\mathbf{r})$  (third-order

derivative of electron density with respect to the applied electric fields), is defined based on the expression

$$\gamma = -\frac{1}{3!} \int r \rho^{(3)}(\mathbf{r}) d^3r = -\frac{1}{3!} \int r \frac{\partial^3 \rho(\mathbf{r})}{\partial F^3} \Big|_{F=0} d^3r \quad (4)$$

The positive and negative values of  $\rho^{(3)}(\mathbf{r})$  multiplied by  $F^3$  represent the field-induced increase and decrease in the third-order charge density, respectively, and are at the origin of the third-order dipole moment (third-order polarization) in the direction from positive to negative  $\gamma$  densities. The  $\gamma$  densities are calculated for a grid of points by using a numerical third-order differentiation of the electron densities calculated by Gaussian 03. The box dimensions ( $-12 \leq x \leq 12$  Å,  $-12 \leq z \leq 12$  Å and  $-5.0 \leq y \leq 5.0$  Å) ensure that the  $\gamma$  values obtained by integration are within 1% of the FF results. The relationship between  $\gamma$  and  $\rho^{(3)}(\mathbf{r})$  is explained by considering the example of a pair of localized  $\gamma$  densities with positive and negative values: the sign of the contribution to  $\gamma$  is positive when the direction from positive to negative  $\gamma$  density coincides with the positive direction of the coordinate system and vice versa. The magnitude of the contribution associated with this pair of  $\gamma$  densities is proportional to the distance between them.

### 3. Results and Discussion

**3.1. Effect of Central Ring Modification on  $\gamma$ .** Table 1 reports the  $\gamma$  values, the diradical characters, the NICS(1) of the central ring, as well as different HOMO–LUMO gaps, the average bond-length alternations (BLAs), and the Mulliken charges on the phenalenyl ring for compounds 1–11 in comparison with compound 12. The NICS(1)s, which correspond to minus the absolute magnetic shielding calculated 1 Å above the ring plane,<sup>26,37</sup> were taken from ref 37. They were calculated by the GIAO/HF/6-311+G\*\* method, using geometries optimized at the MP2(fc)/6-311+G\*\* level of approximation. Rings with negative (positive) NICS(1) values are aromatic (antiaromatic), and the more negative (positive) the NICS(1)s, the more aromatic (antiaromatic) the rings are.



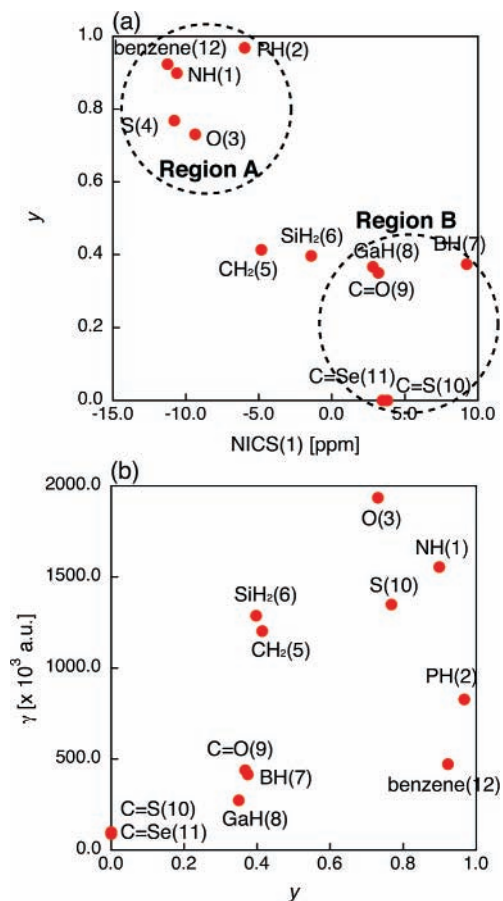


**Figure 2.** Relationship between NICS(1) [ppm] and diradical character ( $y$ ) (a) and relationship between  $y$  and  $\gamma$  [a.u.] (b) for compounds 1–12.

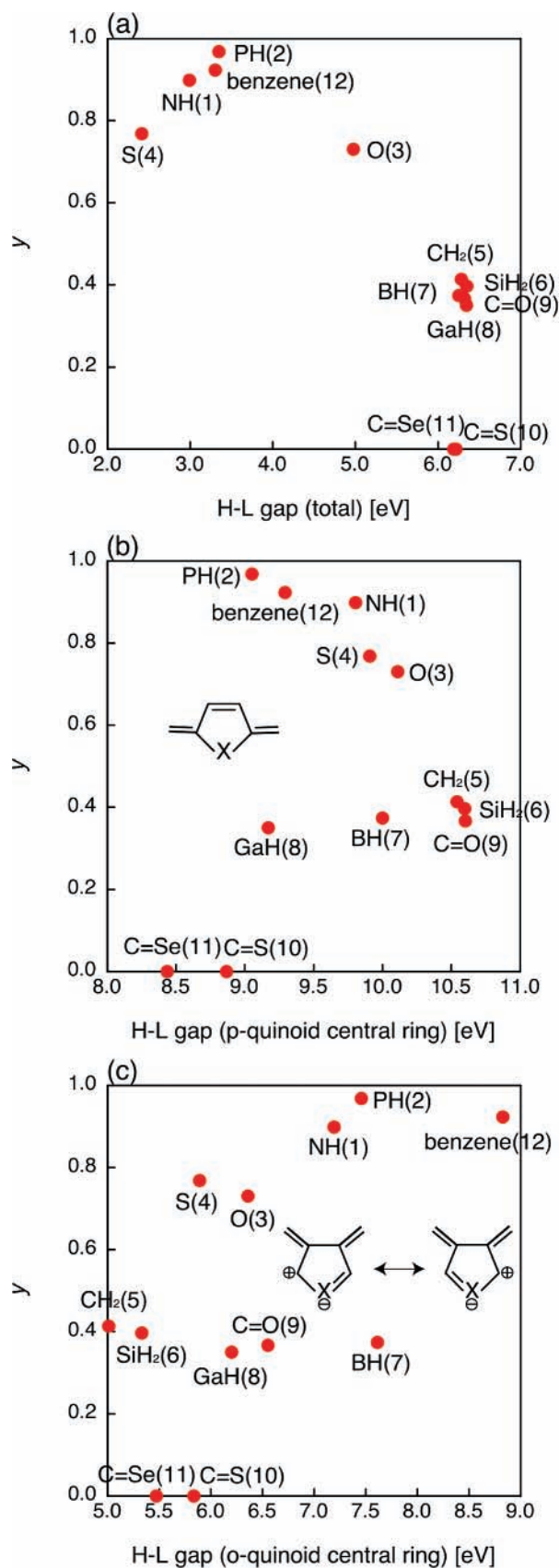
Figure 2a shows the correlation between NICS(1) and  $y$  for 1–12. Region A is characterized by central rings with large and negative NICS(1) and compounds with diradical character larger than 0.7 whereas region B encompasses rings with positive NICS(1) and systems with  $y < 0.4$ . In the former, the lone pair of the X group participates in the electronic delocalization leading to aromatic stabilization whereas in the latter, antiaromaticity is induced by the presence of the X group, which contains a vacant p-orbital (Ga and B atoms) or a positive C atom (C=O, C=S, and C=Se). These electronic features are corroborated by the geometrical structures. In particular, an average bond length alternation (BLA) was determined for characterizing the phenalenyl rings by averaging the absolute values of the CC bond length differences between consecutive bonds. This average BLA is indeed smaller in compounds 1–4 (0.015 to 0.023 Å) and 12 (*as-IDPL*, 0.013 Å), figuring out a stronger contribution of the diradical form I (Figure 1) than in the compounds with smaller aromaticity or antiaromaticity (average BLA = 0.034–0.036 Å). The two remaining species with a  $sp^3$  hybridization of the X group [X = CH<sub>2</sub> (5), SiH<sub>2</sub> (6)] present intermediate properties: small negative NICS(1) and  $y \approx 0.4$ . This suggests that the diradical character of the DPL-based compounds can be controlled to some extent by the aromaticity of the central ring. The correlation between the diradical character and the aromaticity of the central ring is thus related to the description of the electronic structure by three dominant resonance forms: diradical I (involving the central aromatic ring), quinoid (closed-shell) II (involving the central antiaromatic ring), and zwitterionic (closed-shell) III (involving the central antiaromatic ring) shown in Figure 1. For instance, going from compound 1 to 3, the aromaticity is reduced, the

average BLA in the phenalenyl rings increases, the negative charge on the central ring increases, and the diradical character decreases. The same relationship between  $y$ , the charge, and the BLA is found between compounds 2 and 4, whereas compound 5 presents a larger NICS amplitude, a smaller charge separation, and a slightly larger  $y$  value than compound 6. The difference between 9 on the one hand and, on the other hand, 10 and 11 can be found in the larger zwitterionic contribution, revealed by the larger negative charge on the central ring.

The relationship between  $y$  and  $\gamma$  is shown in Figure 2b. Although the variations in  $\gamma$  are not fully accounted for by the values of  $y$ , the usual trend observed in symmetric diradical species is globally reproduced, i.e., an increase of  $\gamma$  with  $y$  until a maximum is reached for intermediate diradical character and then a decrease of  $\gamma$  toward larger  $y$  values. Consequently, compounds 7–11 having the smallest  $y$  values present  $\gamma$  values between about  $100 \times 10^3$  and  $500 \times 10^3$  au, in compounds 3–6  $\gamma$  increases up to about  $2000 \times 10^3$  au, while for compounds 1, 2, and 12,  $\gamma$  gets smaller again.

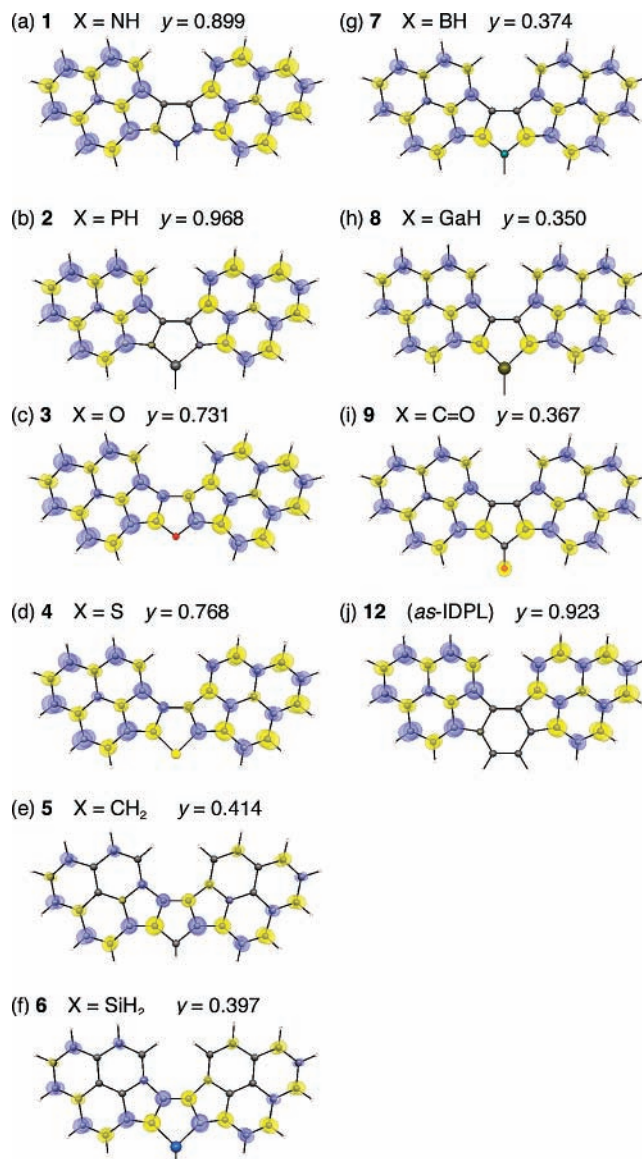
To search for further insight into these variations of  $\gamma$  and  $y$ , HOMO–LUMO energy gaps were considered as possible indicators, for the full systems as well as for their central moieties adopting *p*-*o*-quinoid forms. The HOMO–LUMO energy gaps were calculated at the RHF/6-31G\* level of approximation by using the structures optimized by the UB3LYP/6-31G\*\* method. Referring to the *p*-quinodimethane model where the HOMO–LUMO gap decreases with increasing aromaticity of the central ring, the  $y$  value is expected to be larger for smaller HOMO–LUMO gaps. Then, the *o*-quinoid form of the five-membered rings presents a zwitterionic contribution (resonance form III in Figure 1), which is consistent with a smaller HOMO–LUMO gap than for the *p*-quinoid structure, as shown in Table 1.<sup>38</sup> Although complex, Figure 3 displays some trends between  $y$  and the HOMO–LUMO gaps. In Figure 3a, the systems with the aromatic rings and large  $y$  values present a small HOMO–LUMO gap, whereas in this family, the larger the gap, the smaller the diradical character is. Most of the other systems have a gap ranging between 6.2 and 6.4 eV while  $0 \leq y \leq 0.414$ . In Figure 3b, for compounds of region A, a decrease of the diradical character is accompanied by a reduction of the HOMO–LUMO gap of the *p*-quinoid species whereas for the other species, the trend is opposite. In other words, the H–L gap of the *p*-quinoid species and  $\gamma$  present a similar dependence in  $y$ : an increase until a maximum is attained for intermediate diradical character and then a decrease. Moreover, one can hardly observe a clear correlation between the diradical characters and the gaps of the *o*-quinoid species (Figure 3c). This further indicates that the HOMO–LUMO energy gaps of the total systems are not only determined by the contribution of the central *p*-*o*-quinoid forms but also by both diphenalenyl rings.

Figure 4 shows the  $\alpha$ - and  $\beta$ -spin density distributions for the open-shell systems (at the UBHandHLYP/6-31G\* level of approximation), 1–9 and 12. For systems with an aromatic central ring, the spin density distributions on the left- and right-hand sides are mirror images but with opposite sign so that spin polarization occurs between the two phenalenyl rings and the central ring presents a resulting zero spin density. In the singlet state, the spatial distributions of the  $\alpha$  and  $\beta$  spins are symmetry-broken (spin-polarized). For 1 ( $y = 0.899$ ), 2 ( $y = 0.968$ ), and 12 ( $y = 0.923$ ), whose diradical characters are close to 1, the primary  $\alpha$  and  $\beta$  spin densities are well separated on the right- and left-hand side phenalenyl rings, respectively, though spin polarization is also observed in the phenalenyl rings and the



**Figure 3.** Relationship between diradical character ( $y$ ) and HOMO(L)–LUMO(L) energy gaps [eV] of full compounds (a), of the corresponding *p*-quinoid (b), and of *o*-quinoid (c) rings of 1–12. The structures of the *p*- and *o*-quinoid rings are provided in the inset.

degree of separation for **1** is slightly smaller than that for **2** and **12**. For **3** ( $y = 0.731$ ) and **4** ( $y = 0.768$ ), we observe significant



**Figure 4.** Spin density distributions of 1–9 and 12 calculated at the UBHandHLYP/6-31G\* level of approximation together with their diradical characters. The yellow and blue meshes represent  $\alpha$  and  $\beta$  spin densities with isosurface 0.01 au, respectively.

spin density distribution on the central ring, indicating that the separation between the  $\alpha$  and  $\beta$  spin densities is smaller than that for **1**, **2**, and **12**. Furthermore, in **5** ( $y = 0.414$ ) and **6** ( $y = 0.397$ ) the spin densities are larger on the central ring than on the diphenalenyl rings, indicating further smaller separation between the  $\alpha$  and  $\beta$  spin densities. In contrast, when the central ring is antiaromatic, the spin density distribution is perfectly symmetric along the longitudinal  $x$ -axis and the spin polarization occurs between the diphenalenyl rings and the central ring. This situation appears for **7** ( $y = 0.374$ ), **8** ( $y = 0.350$ ), and **9** ( $y = 0.367$ ), which display a  $y$  value slightly smaller than in compounds **5** and **6**.

Figure 5 shows the  $\gamma$  density distributions for 1–12 at the BHandHLYP/6-31G\* level of approximation, in which spin-restricted solutions are obtained for **10** and **11**, while spin-unrestricted solutions for others. For all systems, the primary contributions to  $\gamma$  are found to arise from  $\pi$ -electrons though  $\sigma$ -electrons provide small opposite contributions to  $\gamma$ . For **1**–**6**, we observe extended positive and negative  $\gamma$  densities well separately distributed on the left and right phenalenyl radical



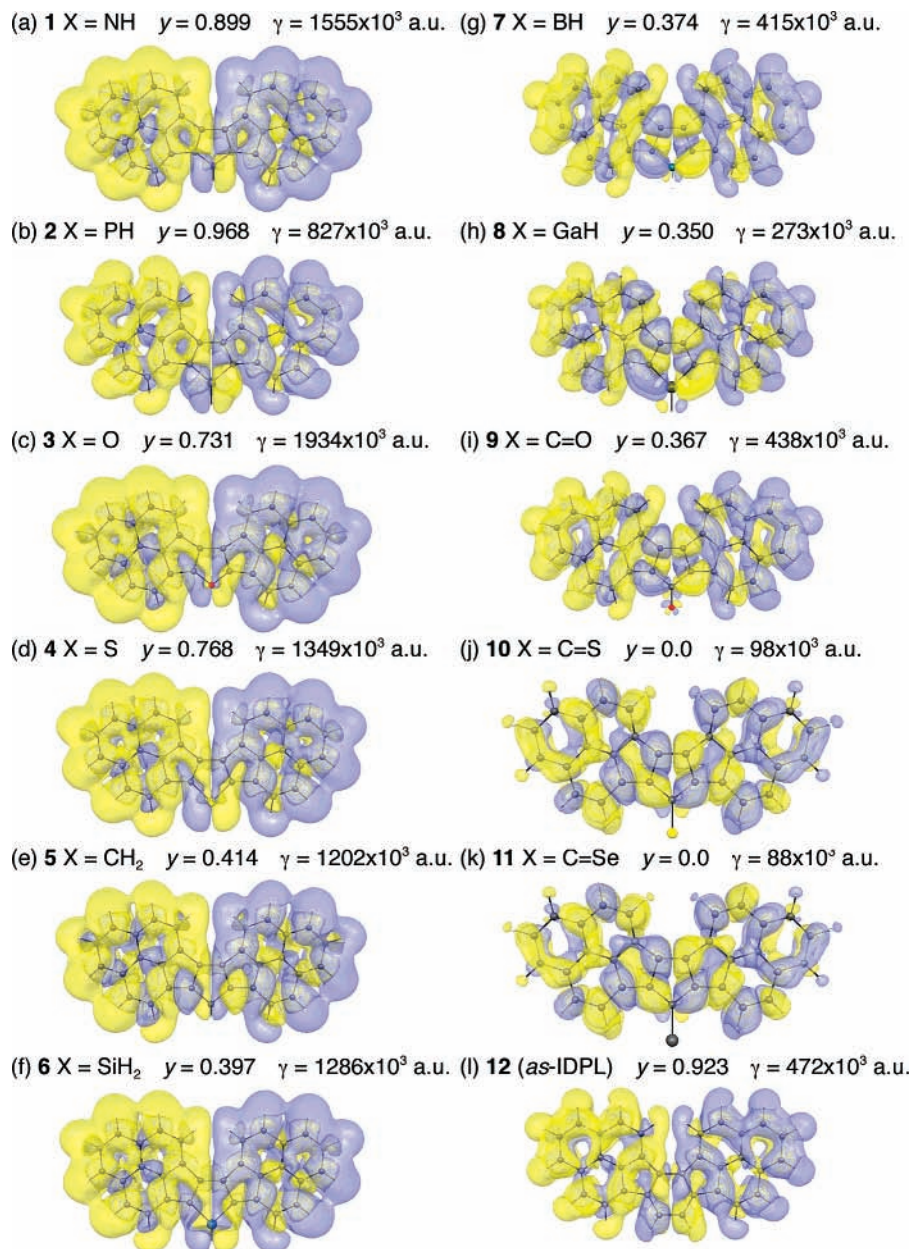


**Figure 5.**  $\gamma$  density distributions of **1**–**12** calculated at the UBHandHLYP/6-31G\* level of approximation. The yellow and blue meshes represent positive and negative  $\gamma$  densities with isosurface  $\pm 100$  au, respectively.

rings, respectively, which provide dominant positive contribution to  $\gamma$  though slight opposite (negative) contribution appears in the central region. The patterns of these  $\gamma$  density distributions are similar to those of other types of diphenalenyl radical systems.<sup>24d,e</sup> For **2** and **12**, which give nearly pure diradical character, the left- and right-hand side  $\gamma$  density regions are more reduced than those of **3**, **4**, **5**, and **6** though the similar well-separated positive and negative  $\gamma$  density regions are observed. The  $\gamma$  density distribution of **1**, which also gives a diradical character close to 1 though it is slightly smaller than those for **2** and **12**, is shown to be somewhat more extended as compared to those of **2** and **12** and to be rather similar to those of **3**–**6**. For **7**–**11**, which are regarded as (nearly) closed-shell systems, on the one hand, the  $\gamma$  densities are reduced and, on the other hand, cancellation of contributions of opposite sign increases when going from **7**–**9** to **10**–**11**. In these cases, the  $\gamma$  densities along the conjugated pathways adopt an alternating pattern similar to conventional closed-shell polyenic systems.<sup>10</sup>

**TABLE 2: The Diradical Characters ( $y$ ) and  $\gamma$  Values of **9** (X = C=O, Y<sub>1</sub>=H, Y<sub>2</sub>=H), **13** (X = C=O, Y<sub>1</sub>=NH<sub>2</sub>, Y<sub>2</sub>=H), **14** (X = C=O, Y<sub>1</sub>=H, Y<sub>2</sub>=NH<sub>2</sub>), **15** (X = C=O, Y<sub>1</sub>=NO<sub>2</sub>, Y<sub>2</sub>=H), and **16** (X = C=O, Y<sub>1</sub>=H, Y<sub>2</sub>=NO<sub>2</sub>)**

system	Y <sub>1</sub>	Y <sub>2</sub>	$y^a$	$\gamma^b$ [ $\times 10^3$ au]
<b>9</b>	H	H	0.367	438
<b>13</b>	NH <sub>2</sub>	H	0.0	164
<b>14</b>	H	NH <sub>2</sub>	0.0	158
<b>15</b>	NO <sub>2</sub>	H	0.366	367
<b>16</b>	H	NO <sub>2</sub>	0.367	358

<sup>a</sup> The  $y$  values are calculated from the UNO/6-31G\* results. <sup>b</sup> The  $\gamma$  values are calculated by the (U)BHandHLYP/6-31G\* method.

These amplitudes of the  $\gamma$  densities are consistent with the amplitude of the  $\gamma$  values.

**3.2. Effect on  $\gamma$  of the Donor and Acceptor Substitutions to the Phenalenyl Rings of Compound **9**.** Table 2 lists the BHandHLYP/6-31G\*  $\gamma$  values of four types of donor (–NH<sub>2</sub>) and acceptor (–NO<sub>2</sub>) disubstituted systems [DPLs with X = O and (Y<sub>1</sub>, Y<sub>2</sub>) = (NH<sub>2</sub>, H) (**13**), (H, NH<sub>2</sub>) (**14**), (NO<sub>2</sub>, H) (**15**),

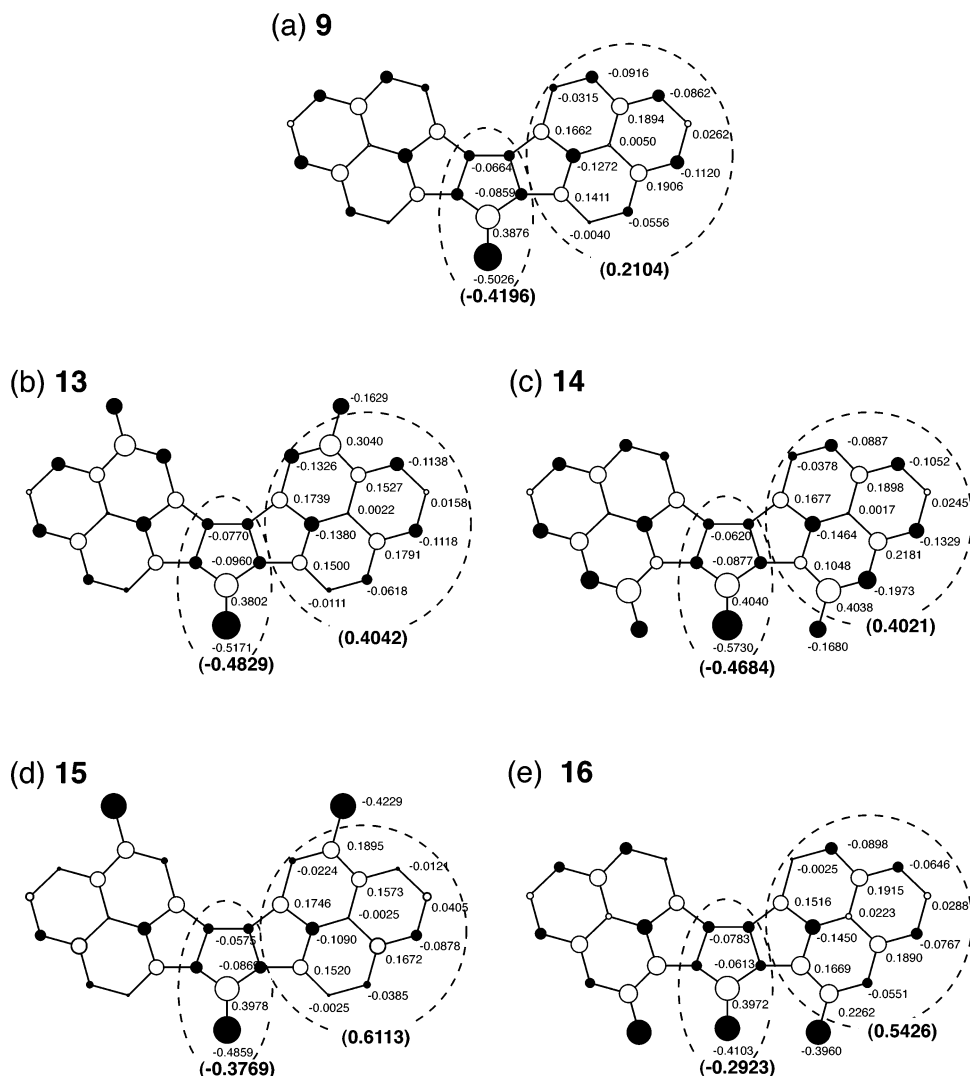


**Figure 6.** Mulliken charge distributions of **9** (a), **13** [b, X = C=O, (Y<sub>1</sub>,Y<sub>2</sub>) = (NH<sub>2</sub>, H)], **14** [c, X = C=O, (Y<sub>1</sub>,Y<sub>2</sub>) = (H, NH<sub>2</sub>)], **15** [d, X = C=O, (Y<sub>1</sub>,Y<sub>2</sub>) = (NO<sub>2</sub>, H)], and **16** [e, X = C=O, (Y<sub>1</sub>,Y<sub>2</sub>) = (H, NO<sub>2</sub>)] calculated by the (U)BHandHLYP/6-31G\* method. The values in parentheses indicate the sum of charges in the central and phenalenyl ring regions.

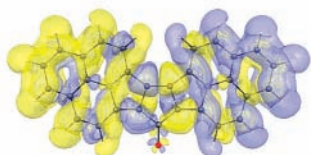
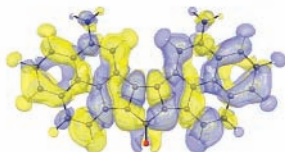
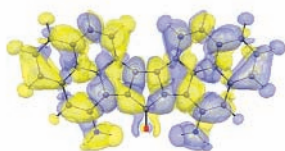
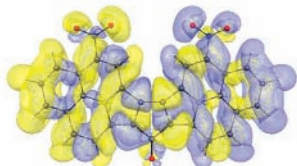
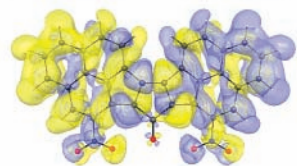
(H, NO<sub>2</sub>) (**16**), Figure 1] in comparison with the reference nonsubstituted system **9**. We still focus on the longitudinal component (in the direction *x*) of  $\gamma$  because our purpose is to clarify the relationships between the radical separation (diradical character) on both-end phenalenyl rings and  $\gamma$  though the perpendicular components (in the direction *y*) of  $\gamma$  might be larger than the longitudinal components for specific combinations of donor/acceptor substitutions.

First, the  $\gamma$  values of donor-substituted systems **13** ( $\gamma = 164 \times 10^3$  au) and **14** ( $\gamma = 158 \times 10^3$  au) are much reduced relative to these of the nonsubstituted system **9** ( $\gamma = 438 \times 10^3$  au), which originates in their closed-shell nature ( $\gamma = 0.0$ ). The combination of C=O group in the central five-membered ring and donor (–NH<sub>2</sub>) groups substituted to diphenalenyl rings increases in fact the contribution of charge separated (zwitterionic) closed-shell forms (Figure 1). This is exemplified by the Mulliken charge distributions of these systems shown in Figure 6: for **9**, the Mulliken charges on the central and both-end phenalenyl rings amount to –0.42 and 0.42, respectively, whereas for **13** (**14**) the Mulliken charges on the central and both-end phenalenyl rings amount to –0.48 (–0.47) and 0.81 (0.80), respectively. On the other hand, the introduction of acceptor (–NO<sub>2</sub>) groups into diphenalenyl rings, **15** ( $\gamma = 0.366$ ) and **16** ( $\gamma = 0.367$ ), hardly changes the diradical character as

compared to the nonsubstituted system **9** ( $\gamma = 0.367$ ) while it enhances the positive charge on the diphenalenyl rings and reduces the negative charge on the central ring relative to nonsubstituted system **9**. In this case, the charge contrast between the diphenalenyl and central ring is larger than in **9**, but the diradical character remains similar. Moreover, the  $\gamma$  values of compounds **15** and **16** are close to that of compound **9**. From Figure 7, **13** and **14** show similar  $\gamma$  density distributions, demonstrating a further reduction of the  $\gamma$  densities relative to that of nonsubstituted system **9** as well as an alternating, partially cancelled,  $\gamma$  density. Sign alternating  $\gamma$  density is also observed for **15** and **16**, whose  $\gamma$  density distributions are similar to those of **9** except for the substituent group regions. These features corroborate the relative magnitudes of  $\gamma$  among **9** and **13**–**16**.

#### 4. Conclusions

The relationship between the second hyperpolarizability and the diradical character has been theoretically investigated for diphenalenyl-based compounds containing different heterocyclic five-membered central rings or substituted by donor/acceptor groups. The calculations have been performed adopting density functional theory and a hybrid exchange–correlation functional including 50% of Hartree–Fock exchange, which was demon-

(a) **9**  $\gamma = 0.367$   $\gamma = 438 \times 10^3$  a.u.(b) **13**  $\gamma = 0.0$   $\gamma = 164 \times 10^3$  a.u.(c) **14**  $\gamma = 0.0$   $\gamma = 158 \times 10^3$  a.u.(d) **15**  $\gamma = 0.366$   $\gamma = 367 \times 10^3$  a.u.(e) **16**  $\gamma = 0.367$   $\gamma = 358 \times 10^3$  a.u.

**Figure 7.**  $\gamma$  density distributions of **9** (a), **13** (b), **14** (c), **15** (d) and **16** (e) (see Figure 1) calculated by the (U)BHandHLYP/6-31G\* method. The yellow and blue meshes represent positive and negative  $\gamma$  densities with isosurface  $\pm 100$  au, respectively.

strated several times to reproduce, at least qualitatively, the  $\gamma$  values determined at the highly correlated coupled-clusters level of approximation.

When the central ring is strongly aromatic, the diradical character is larger than 0.7, which is associated with pretty large  $\gamma$  values except for almost the pure diradical case ( $\gamma \approx 1$ ). When the aromaticity decreases—or the antiaromaticity increases—the diradical character and the second hyperpolarizability get smaller. These relationships can be correlated with structural (bond length alternation) and charge distribution (charge transfer between the phenalenyl rings and the central ring) properties, which account for the relative importance of the resonance diradical, zwitterionic, and quinoid forms. These results suggest that diradical character and the second hyperpolarizability can be controlled by the aromaticity of the ring while the paradigm of the enhancement of  $\gamma$  for intermediate diradical character<sup>23–24</sup> is globally verified. Nevertheless, the relationship between  $\gamma$  and  $\gamma$  appears to be more complex—and influenced by other parameters—than for the model dissociating H<sub>2</sub> and *p*-quinodimethane compounds. Furthermore, some complex relationships between the HOMO–LUMO gap,  $\gamma$ , and  $\gamma$  have been evidenced, in particular with the HOMO–LUMO gap of the constituting *p*-quinoid structures.

Introducing donor (–NH<sub>2</sub>) and acceptor (–NO<sub>2</sub>) groups on the phenalenyl rings leads to distinct effects. In the case of

substitutions by donors, the charge transfer and zwitterionic character is enhanced, leading to closed-shell species and small second hyperpolarizabilities. In the other case, the charge transfer is reduced but the diradical character and the second hyperpolarizability hardly changes.

In summary, by using different five-membered heterocycles or donor/acceptor groups, the diradical character of diphenalenyl-based compounds has been varied from 0.0 to 0.968, leading to a variation of  $\gamma$  over more than 1 order of magnitude, demonstrating the controllability of  $\gamma$  in this family of compounds. The present results, therefore, will be applicable to the rational design of substances with desired NLO properties through the chemical modification of central atoms in five-membered rings and/or substituent groups to diphenalenyl rings in these diphenalenyl diradical systems.

**Acknowledgment.** This work was supported by Grant-in-Aid for Scientific Research (No. 18350007) from the Japan Society for the Promotion of Science (JSPS) and a Grant-in-Aid for Scientific Research on Priority Areas (No.18066010) from the Ministry of Education, Science, Sports and Culture of Japan, and the global COE (center of excellence) program “Global Education and Research Center for Bio-Environmental Chemistry” of Osaka University. B.C. thanks the Belgian National Fund for Scientific Research for his Research Director position. E.B. thanks the Interuniversity Attraction Pole on “Supramolecular Chemistry and Supramolecular Catalysis” (IUAP No. P6-27) for her postdoctoral grant.

**Supporting Information Available:** Bond lengths on phenalenyl rings for **1–12** as well as IDPL, *as*-IDPL, and isolated phenalenyl ring optimized by the UB3LYP/6-31G\*\* method, and Mulliken charge densities for **1–12**. This material is available free of charge via the Internet at <http://pubs.acs.org>.

## References and Notes

- Pathenopoulos, D. A.; Rentzepis, P. M. *Science* **1989**, *245*, 893.
- Albota, M.; Beljonne, D.; Brédas, J. L.; Herlich, J. E.; Fu, J. Y.; Heikal, A. A.; Hess, S.; Kogej, T. E.; Levin, M. D.; Marder, S. R.; McCord-Maughon, D.; Perry, J. W.; Rockel, H.; Rumi, M.; Subramanian, G.; Webb, W. W.; Wu, X. L.; Xu, C. *Science* **1998**, *281*, 1653.
- Zhou, W.; Kuebler, S. M.; Braun, K. L.; Yu, T.; Cammack, J. K.; Ober, C. K.; Perry, J. W.; Marder, S. R. *Science* **2002**, *296*, 1106.
- Kawata, S.; Sun, H.-B.; Tanaka, T.; Takada, T. *Nature* **2001**, *412*, 697.
- He, G. S.; Bhawalker, J. D.; Zhao, C. F.; Prasad, P. N. *Appl. Phys. Lett.* **1995**, *67*, 2433.
- Parthenopoulos, D. A.; Rentzepis, P. M. *Science* **1989**, *245*, 843.
- Frederiksen, P. K.; Jørgensen, M.; Ogilby, P. R. *J. Am. Chem. Soc.* **2001**, *123*, 1215.
- de Melo, C. P.; Silbey, R. *Chem. Phys. Lett.* **1987**, *140*, 537.
- Nakano, M.; Yamaguchi, K. *Chem. Phys. Lett.* **1993**, *206*, 285.
- (a) Nakano, M.; Shigemoto, I.; Yamada, S.; Yamaguchi, K. *J. Chem. Phys.* **1995**, *103*, 4175. (b) Nakano, M.; Yamaguchi, K.; Fueno, T. *Chem. Phys. Lett.* **1991**, *185*, 550.
- Nakano, M.; Kiribayashi, S.; Yamada, S.; Shigemoto, I.; Yamaguchi, K. *Chem. Phys. Lett.* **1996**, *262*, 66.
- de Melo, C. P.; Fonseca, T. L. *Synth. Met.* **1997**, *85*, 1085.
- de Melo, C. P.; Fonseca, T. L. *Chem. Phys. Lett.* **1996**, *28*, 28.
- Kirtman, B.; Champagne, B. *Int. Rev. Phys. Chem.* **1997**, *16*, 389.
- Yamada, S.; Nakano, M.; Shigemoto, I.; Kiribayashi, S.; Yamaguchi, K. *Chem. Phys. Lett.* **1997**, *267*, 438.
- Champagne, B.; Deumens, E.; Öhrn, Y. *J. Chem. Phys.* **1997**, *107*, 5433.
- An, S.; Wong, K. Y. *J. Chem. Phys.* **2001**, *114*, 1010.
- Champagne, B.; Kirtman, B. In *Handbook of Advanced Electronic and Photonic Materials and Devices*; Nalwa, H. S., Ed.; Academic Press: New York, 2001; Vol. 9, p 63.
- Nakano, M.; Fujita, H.; Takahata, M.; Yamaguchi, K. *J. Am. Chem. Soc.* **2002**, *124*, 9648.
- Fujita, H.; Nakano, M.; Takahata, M.; Yamaguchi, K. *Chem. Phys. Lett.* **2002**, *358*, 435.



- (21) Champagne, B.; Spassova, M.; Jadin, J. B.; Kirtman, B. *J. Chem. Phys.* **2002**, *116*, 3935.
- (22) Nakano, M.; Nitta, T.; Yamaguchi, K.; Champagne, B.; Botek, E. *J. Phys. Chem. A* **2004**, *108*, 4105.
- (23) (a) Nakano, M.; Nagao, H.; Yamaguchi, K. *Phys. Rev. A* **1997**, *55*, 1503. (b) Nakano, M.; Yamada, S.; Yamaguchi, K. *J. Comput. Methods Sci. Eng.* **2004**, *4*, 677. (c) Nakano, M.; Yamada, S.; Kishi, R.; Takahata, M.; Nitta, T.; Yamaguchi, K. *J. Nonlinear Opt. Phys. Mater.* **2004**, *13*, 411.
- (24) (a) Nakano, M.; Kishi, R.; Nitta, T.; Kubo, T.; Nakasuji, K.; Kamada, K.; Ohta, K.; Champagne, B.; Botek, E.; Yamaguchi, K. *J. Phys. Chem. A* **2005**, *109*, 885. (b) Nakano, M.; Kishi, R.; Ohta, S.; Takebe, A.; Takahashi, H.; Furukawa, S.; Kubo, T.; Morita, Y.; Nakasuji, K.; Yamaguchi, K.; Kamada, K.; Ohta, K.; Champagne, B.; Botek, E. *J. Chem. Phys.* **2006**, *125*, 74113. (c) Nakano, M.; Kishi, R.; Nakagawa, N.; Ohta, S.; Takahashi, H.; Furukawa, S.; Kamada, K.; Ohta, K.; Champagne, B.; Botek, E.; Yamada, S.; Yamaguchi, K. *J. Phys. Chem. A* **2006**, *110*, 4238. (d) Nakano, M.; Kubo, T.; Kamada, K.; Ohta, K.; Kishi, R.; Ohta, S.; Nakagawa, N.; Takahashi, H.; Furukawa, S.; Morita, Y.; Nakasuji, K.; Yamaguchi, K. *Chem. Phys. Lett.* **2005**, *418*, 142. (e) Ohta, S.; Nakano, M.; Kubo, T.; Kamada, K.; Ohta, K.; Kishi, R.; Nakagawa, N.; Champagne, B.; Botek, E.; Umezaki, S.; Takebe, A.; Takahashi, H.; Furukawa, S.; Morita, Y.; Nakasuji, K.; Yamaguchi, K. *Chem. Phys. Lett.* **2005**, *420*, 432. (f) Nakano, M.; Nakagawa, N.; Ohta, S.; Kishi, R.; Kubo, T.; Kamada, K.; Ohta, K.; Champagne, B.; Botek, E.; Takahashi, H.; Furukawa, S.; Morita, Y.; Nakasuji, K.; Yamaguchi, K. *Chem. Phys. Lett.* **2006**, *429*, 174. (g) Champagne, B.; Botek, E.; Nakano, M.; Nitta, T.; Yamaguchi, K. *J. Chem. Phys.* **2005**, *122*, 114315. (h) Champagne, B.; Botek, E.; Quinet, O.; Nakano, M.; Kishi, R.; Nitta, T.; Yamaguchi, K. *Chem. Phys. Lett.* **2005**, *407*, 372. (i) Ohta, S.; Nakano, M.; Kubo, T.; Kamada, K.; Ohta, K.; Kishi, R.; Nakagawa, N.; Champagne, B.; Botek, E.; Takebe, A.; Umezaki, S.; Nate, M.; Takahashi, H.; Furukawa, S.; Morita, Y.; Nakasuji, K.; Yamaguchi, K. *J. Phys. Chem. A* **2007**, *111*, 3633.
- (25) Kamada, K.; Ohta, K.; Kubo, T.; Shimizu, A.; Morita, Y.; Nakasuji, K.; Kishi, R.; Ohta, S.; Furukawa, S.; Takahashi, H.; Nakano, M. *Angew. Chem., Int. Ed.* **2007**, *16*, 3544.
- (26) Schleyer, P. v. R.; Maerker, C.; Dransfield, A.; Jiao, H.; Hommes, N. J. R. v. E. *J. Am. Chem. Soc.* **1996**, *118*, 6317.
- (27) Herebian, D.; Wieghardt, K. E.; Neese, F. *J. Am. Chem. Soc.* **2003**, *125*, 10997.
- (28) (a) Kubo, T. Doctorial thesis, Osaka University, 1996. (b) Kubo, T.; Shimizu, A.; Uruichi, M.; Yakushi, K.; Nakano, M.; Shiomi, D.; Sato, K.; Takui, T.; Morita, Y.; Nakasuji, K. *Org. Lett.* **2007**, *9*, 81.
- (29) Yamaguchi, K. *Self-Consistent Field: Theory and Applications*; Carbo, R., Klobukowski, M., Eds.; Elsevier: Amsterdam, The Netherlands, 1990; p 727.
- (30) Yamanaka, S.; Okumura, M.; Nakano, M.; Yamaguchi, K. *J. Mol. Struct. (THEOCHEM)* **1994**, *310*, 205.
- (31) Frisch, M. J.; Trucks, G. W.; Schlegel, H. B.; Scuseria, G. E.; Robb, M. A.; Cheeseman, J. R.; Montgomery, J. A., Jr.; Vreven, T.; Kudin, K. N.; Burant, J. C.; Millam, J. M.; Iyengar, S. S.; Tomasi, J.; Barone, V.; Mennucci, B.; Cossi, M.; Scalmani, G.; Rega, N.; Petersson, G. A.; Nakatsuji, H.; Hada, M.; Ehara, M.; Toyota, K.; Fukuda, R.; Hasegawa, J.; Ishida, M.; Nakajima, T.; Honda, Y.; Kitao, O.; Nakai, H.; Klene, M.; Li, X.; Knox, J. E.; Hratchian, H. P.; Cross, J. B.; Bakken, V.; Adamo, C.; Jaramillo, J.; Gomperts, R.; Stratmann, R. E.; Yazyev, O.; Austin, A. J.; Cammi, R.; Pomelli, C.; Ochterski, J. W.; Ayala, P. Y.; Morokuma, K.; Voth, G. A.; Salvador, P.; Dannenberg, J. J.; Zakrzewski, V. G.; Dapprich, S.; Daniels, A. D.; Strain, M. C.; Farkas, O.; Malick, D. K.; Rabuck, A. D.; Raghavachari, K.; Foresman, J. B.; Ortiz, J. V.; Cui, Q.; Baboul, A. G.; Clifford, S.; Cioslowski, J.; Stefanov, B. B.; Liu, G.; Liashenko, A.; Piskorz, P.; Komaromi, I.; Martin, R. L.; Fox, D. J.; Keith, T.; Al-Laham, M. A.; Peng, C. Y.; Nanayakkara, A.; Challacombe, M.; Gill, P. M. W.; Johnson, B.; Chen, W.; Wong, M. W.; Gonzalez, C.; Pople, J. A. *Gaussian 03*, Revision C.02; Gaussian, Inc.: Wallingford, CT, 2004.
- (32) Hurst, G. J. B.; Dupuis, M.; Clementi, E. *J. Chem. Phys.* **1988**, *89*, 385.
- (33) Maroulis, G. J. *J. Chem. Phys.* **1999**, *111*, 583.
- (34) Maroulis, G. J.; Xenides, D.; Hohm, U.; Loose, A. *J. Chem. Phys.* **2001**, *115*, 7957.
- (35) Cohen, H. D.; Roothaan, C. C. J. *J. Chem. Phys.* **1965**, *43*, S34.
- (36) Willetts, A.; Rice, J. E.; Burland, D. M.; Shelton, D. P. *J. Chem. Phys.* **1992**, *97*, 7590.
- (37) Cyrański, M. K.; Krygowski, T. M.; Katritzky, A. R.; Schleyer, P. v. R. *J. Org. Chem.* **2002**, *67*, 1333.
- (38) The HOMO-LUMO energy gaps of *o*-xylylene and *p*-dimethylenethiophene reported in a previous paper<sup>24f</sup> are revised as 8.828 and 9.292 eV, respectively.